Journal of Zhejiang University-SCIENCE B (Biomedicine & Biotechnology) 2021 22(10):839-855
www.jzus.zju.edu.cn; www.springer.com/journal/11585
E-mail: jzus_b@zju.edu.cn

Research Article
https://doi.org/10.1631/jzus.B2000802

Check for updates

A proteomic analysis of Bcl-2 regulation of cell cycle arrest: insight into the mechanisms

Xing DU[1,2*], Jingjing XIAO[1,3*], Xufeng FU[1,2], Bo XU[1], Hang HAN[1], Yin WANG[1,3✉], Xiuying PEI[1✉]

[1]*Key Laboratory of Fertility Preservation and Maintenance of Ministry of Education, Ningxia Medical University, Yinchuan 750004, China*
[2]*Department of Biochemistry and Molecular Biology, Ningxia Medical University, Yinchuan 750004, China*
[3]*Department of Physiology and Neurobiology, Ningxia Medical University, Yinchuan 750004, China*

Abstract: B cell lymphoma 2 (*Bcl-2*) is an important antiapoptotic gene that plays a dual role in the maintenance of the dynamic balance between the survival and death of cancer cells. In our previous study, Bcl-2 was shown to delay the G0/G1 to S phase entry by regulating the mitochondrial metabolic pathways to produce lower levels of adenosine triphosphate (ATP) and reactive oxygen species (ROS). However, the detailed molecular mechanisms or pathways by which Bcl-2 regulates the cell cycle remain unknown. Here, we compared the effects of Bcl-2 overexpression with an empty vector control in the NIH3T3 cell line synchronized by serum starvation, and evaluated the effects using proteomic analysis. The effect of Bcl-2 on cell cycle regulation was detected by monitoring Bcl-2 and p27 expression. The result of subsequent proteomic analysis of Bcl-2 overexpressing cells identified 169 upregulated and 120 downregulated proteins with a 1.5-fold change. These differentially expressed proteins were enriched in a number of signaling pathways predominantly involving the ribosome and oxidative phosphorylation, according to the data of Gene Ontology (GO) and Kyoto Encyclopedia of Genes and Genomes (KEGG) enrichment analyses. These results indicated that Bcl-2 potentially acts at the translation level to influence proteins or enzymes of the respiratory chain or in the ribosome, and thereby regulates the cell cycle. Additionally, differentially expressed proteins involved in oxidative phosphorylation were determined to account for most of the effects of Bcl-2 on the cell cycle mediated by the mitochondrial pathway investigated in our previous study. These results can provide assistance for additional in-depth studies on the regulation of the cell cycle by Bcl-2. The results of the proteomic analysis determined the mechanism of Bcl-2-dependent delay of the cell cycle progression. In summary, the results of this study provide a novel mechanistic basis for identifying the key proteins or pathways for designing and developing precisely targeted cancer drugs.

Key words: Cell cycle; B cell lymphoma 2 (Bcl-2); Proteomics; Oxidative phosphorylation

1 Introduction

B cell lymphoma 2 (*Bcl-2*) is an important anti-apoptotic gene that was originally identified in B-cell lymphoma (Jardim et al., 2020). The Bcl-2 family members include antiapoptotic proteins (Bcl-2, Bcl-2-like 2 (Bcl-w), Bcl-2-like 1 (Bcl-xL), Bcl-2-related protein A1 (Bfl-1), and myeloid cell leukemia-1 (Mcl-1)), pro-apoptotic pore-formers (Bcl-2-associated X (Bax), Bcl-2-related ovarian killer protein (Bok), and Bcl-2 homologous antagonist killer (Bak)), and pro-apoptotic BH3-only proteins (Bcl-2-associated agonist of cell death (Bad), BH3-interacting domain death agonist (Bid), Bcl-2-interacting killer (Bik), Bcl-2-like 11 (Bim), Bcl-2-modifying factor (Bmf), Harakiri (Hrk), phorbol-12-myristate-13-acetate-induced protein 1 (Noxa), and Bcl-2-binding component 3 (Puma)), which are classified according to their shared carboxyl terminus transmembrane region and Bcl-2 homologous structure domains BH1–BH4 (Adams et al., 2019). Bcl-2 family proteins work together with other proteins to maintain a dynamic balance between the survival and death of cells (Singh et al., 2019). In response to death signals, pro-apoptotic Bcl-2 members accumulate in the mitochondrial outer membrane, resulting in permeabilization of the membrane and subsequent release

✉ Yin WANG, yin-wang@hotmail.com
Xiuying PEI, peixiuying@163.com
* The two authors contributed equally to this work
Xing DU, https://orcid.org/0000-0003-2683-4524
Xiuying PEI, https://orcid.org/0000-0002-4410-8588

Received Dec. 9, 2020; Revision accepted Mar. 11, 2021;
Crosschecked Sept. 2, 2021

of cytochrome C from the mitochondria and caspase activation to induce cell death (Tait and Green, 2010). In addition to their apoptotic role, Bcl-2 family members have non-apoptotic roles, including involvement in the regulation of mitochondrial physiology, endoplasmic reticulum physiology, nuclear processes (cell cycle and DNA damage response), and autophagy (Hatok and Racay, 2016; Gross and Katz, 2017; Pihán et al., 2017; Xu and Qin, 2019). Note that Bcl-2 can restrain the entry of quiescent cells into the cell cycle and hasten the withdrawal of proliferating cells from the cell cycle. Intriguingly, the function of Bcl-2 in regulation of the cell cycle has been shown to be genetically separate from its prosurvival role (Brady et al., 1996; Vairo et al., 1996). It has been demonstrated that Bcl-2 plays an important dual role and can be a tumor suppressor and an oncogene in various types of human cancer (Zhou et al., 2011; Warren et al., 2019; Xie et al., 2020). Induction of cell cycle arrest and apoptosis is important strategies for antitumor cancer therapy (Gao and Liu, 2019). Therefore, Bcl-2 has been extensively studied as a target of cancer therapy. However, the precise mechanisms of its inhibitory effects on the cell cycle and the tumor suppressor function of Bcl-2 remain unclear. Studies have shown that Bcl-2 can inhibit cell proliferation by delaying the G0/G1 to S phase transition (Linette et al., 1996; Janumyan et al., 2003, 2008). The inhibitory effect of Bcl-2 on the cell cycle depends on a cyclin/cyclin-dependent kinase (CDK) inhibitor p27 during the G1 phase. Bcl-2 overexpression in quiescent fibroblasts results in elevated levels of p27. In contrast, cells entering the S phase rapidly lower their levels of p27, suggesting that p27 can be considered a marker of the G0/G1 to S phase transition (Quinn and Richardson, 2004). Recent studies have revealed the mechanisms by which Bcl-2 regulates the cell cycle through DNA replication stress (Xie et al., 2014, 2020). However, the detailed mechanisms of indirect regulation of the cell cycle by Bcl-2 are unclear.

Numerous studies have investigated drugs-targeting Bcl-2. For example, venetoclax was the first-in-class Bcl-2-specific BH3 mimetic drug to produce barely satisfactory clinical outcomes in cancer therapy (Touzeau et al., 2018). Therefore, the study and development of drugs that target other proteins to inhibit the growth of cancer cells is a new strategy for cancer treatment. Because of the problems of long development time, high costs, and the risks associated with the research and development of new drugs, precise targeting of key cell cycle proteins and signaling pathways plays a critical role in the development and application of new drugs. Proteomic analysis using tandem mass tag (TMT) labeling technology is one of the best methods to investigate complex phenomena at the gene level and can identify dynamic changes in physiological and pathological characteristics in human diseases (Frantzi et al., 2019). Therefore, accurate analysis of target proteins or signaling pathways in heterogeneous tumor samples using TMT-labeled proteomic analysis will contribute to the precise targeted design and development of drugs.

Our previous study demonstrated that Bcl-2 delays the G0/G1 to S phase transition by regulating mitochondrial metabolism to produce less adenosine triphosphate (ATP) and reactive oxygen species (ROS) (Du et al., 2017). Although our findings revealed a novel mechanism of the tumor suppressor function of Bcl-2, the detailed mechanisms of action of the pathways involved in Bcl-2 regulation of the cell cycle and the proteins that influence Bcl-2-dependent regulation of the cell cycle remained unclear. To determine the precise mechanisms of Bcl-2-dependent delay of the G0/G1 to S phase transition, in the present study we compared the Bcl-2-overexpressing NIH3T3 cell line with control vector-treated cells. The cells were synchronized by serum starvation (SS) and subjected to proteomic analysis. The results provide insight into the novel mechanisms of the regulation of cell cycle arrest by Bcl-2.

2 Materials and methods

2.1 Cell lines and cell culture

Mouse embryonic NIH3T3 fibroblasts were purchased from the Shanghai Cell Bank of the Chinese Academy of Sciences (Shanghai, China). NIH3T3 cells were cultured in Dulbecco's modified Eagle's medium (DMEM; Gibco BRL, Grand Island, NY, USA) supplemented with 10% (volume fraction) fetal bovine serum (FBS; Gibco) and 1% (volume fraction) penicillin/streptomycin (Gibco) in an incubator with a humidified atmosphere of 5% CO_2 at 37 °C.

2.2 Western blot analysis

The cell lines transfected with empty vector or the recombinant Bcl-2 plasmid were synchronized in

the G0/G1 phase by SS (0.1% FBS for 48 h) and compared with normally growing (NG) cells. Cells were collected using 2.5 g/L trypsin (Gibco) and washed three times with phosphate-buffered saline (PBS). Then, ice-cold radioimmunoprecipitation assay (RIPA) lysis buffer (Beyotime, Jiangsu, China) containing protease inhibitors was added, and the mixture was incubated on ice for 20 min. After centrifugation at 12 000 r/min for 15 min at 4 ℃, the supernatant was collected and the total protein concentration was quantified using a bicinchoninic acid (BCA) protein assay kit (Beyotime). After incubation at 100 ℃ for 10 min, the protein samples (20 μg/well) were separated by 12.5% (0.125 g/mL) sodium dodecyl sulphate-polyacrylamide gel electrophoresis (SDS-PAGE) and electrotransferred onto polyvinylidene difluoride (PVDF) membranes (EMD Millipore, Billerica, MA, USA) at 100 V constant voltage for 2 h. The membrane was blocked in 0.05 g/mL nonfat milk dissolved in Tris-buffered solution containing Tween 20 (TBST) for 2 h and then incubated with the corresponding primary antibodies (1:1000, volume ratio) at 4 ℃ overnight. After three washes for 5 min with TBST, the membranes were incubated with horseradish peroxidase (HRP)-conjugated secondary antibody for 1 h at room temperature and washed three times with TBST. The signal was detected using an ECL chemiluminescence kit (Thermo Scientific, Boston, USA) in a fluorescence detection device (Fu et al., 2016). Antibodies against Bcl-2 and p27 were purchased from the Cell Signaling Technology Co. (CST, Boston, USA), and an anti-actin antibody was purchased from Beyotime.

2.3 Proteomic analysis

Serum-starved cells were collected for proteomic profiling. The proteomic analysis was performed by PTM Biolabs, Inc. (Hangzhou, China). Briefly, cell samples were sonicated using a high-intensity ultrasonic processor (Scientz, Ningbo, China) in lysis buffer containing 8 mol/L urea and a 0.01 g/mL protease inhibitor cocktail. The remaining cell debris was removed after centrifugation at 12 000 r/min at 4 ℃ for 10 min, and the supernatant was collected and quantified with a BCA kit according to the manufacturer's instructions. Subsequently, protein samples were digested by trypsin after dithiothreitol reduction, iodoacetamide alkylation, and tetraethylammonium bromide dilution. After trypsin digestion, the tryptic peptides were desalted and processed with a TMT kit according to the manufacturer's instructions. The peptides were fractionated using an Agilent 300 Extend C18 column connected to a high pH reverse-phase high-performance liquid chromatography (HPLC) system (Li et al., 2018). The harvested peptides were dissolved in acetonitrile and analyzed using liquid chromatography combined with quadrupole-time of flight tandem mass spectrometry (LC-Q-TOF MS/MS; Thermo Scientific Q Exactive HF-X). The data were analyzed with the MaxQuant search engine (v.1.5.2.8 Max Planck Institute of Biochemistry, Germany) and searched against the human UniProt database for annotation and analysis (Wang et al., 2020). Finally, differentially expressed proteins were analyzed using parallel reaction monitoring technology by PTM Biolabs, Inc., according to the manufacturer's instructions.

2.4 Statistical analysis

For quantitative analysis of protein expression, the quantification of target proteins and β-actin was performed using ImageJ software (NIH, MD, USA). The ratios of the target proteins to β-actin expression are presented as mean±standard deviation (SD) using GraphPad Prism 6 (GraphPad Software, Inc., San Diego, CA, USA). Comparative assessment of various factors was performed by analysis of variance (ANOVA) and unpaired *t*-tests, and a *P*-value of <0.05 was considered statistically significant. Differentially expressed proteins were identified based on a fold change of 1.3 (Bcl-2 vs. control), and a fold change higher than 1.3 or lower than 1/1.3-fold change was considered an upregulated or downregulated trend, respectively, with the *P*-value of <0.05. Comparisons based on a 1.5-fold change were also considered.

Differentially expressed proteins were classified into various categories based on the Gene Ontology (GO) (http://www.ebi.ac.uk/GOA) and Kyoto Encyclopedia of Genes and Genomes (KEGG; http://www.genome.jp/kegg/pathway.html) annotation databases. For each category, a two-tailed Fisher's exact test was applied in the case of all identified differentially expressed proteins. GO and KEGG enrichments with a corrected *P*-value of <0.05 were considered significant. The protein–protein interactions were analyzed using the STRING website (https://string-db.org).

3 Results

3.1 Effects of serum starvation on cell cycle entry

Our previous study showed that Bcl-2 delays cell cycle entry from the G0/G1 to S phases by stabilizing p27 in NIH3T3 and C3H cells synchronized by SS compared with NG cells (Du et al., 2017). In this study, viral vector containing Bcl-2 (referred to as Bcl-2) was used to infect NIH3T3 cells to establish a cell line with stable expression of Bcl-2, and empty vector virus was used as a control. After 48 h of SS, the cells were synchronized at the G0 phase. The result showed that Bcl-2 expression in NIH3T3 cells was stable and not influenced by SS compared to that in the control (Figs. 1b and 1c). An inhibitor of CDK, p27, was also assayed to confirm the synchronization effect of the SS treatment. The results showed that p27 expression was higher in the SS group than in the NG group, and the Bcl-2 group had higher p27 levels than the control group in the SS treatment groups (Figs. 1b and 1d). These results indicated that Bcl-2 can regulate cell cycle entry at the G0/G1 to S phase transition by influencing the expression of p27.

3.2 Analysis of Bcl-2 regulation of cell cycle arrest by proteomics

To investigate the detailed molecular mechanism by which Bcl-2 regulates cell cycle arrest after SS treatment, we used TMT-based proteomics to identify differentially expressed proteins in the control and Bcl-2-overexpressing groups after SS treatment for 48 h. A workflow chart of the quantitative proteomic analysis is shown in Fig. 1a. The quality of the proteomic dataset was confirmed using several indexes, including identified peptide length distribution, protein mass and coverage distribution, principal component analysis (PCA), and Pearson's correlation analysis. As shown in Fig. 2a, most of the peptides included 7–20 amino acids, which is consistent with the general rules for subsequent TMT labeling and quantitative proteomic tests. The protein mass showed a negative correlation with protein sequence coverage (Fig. 2b), because larger

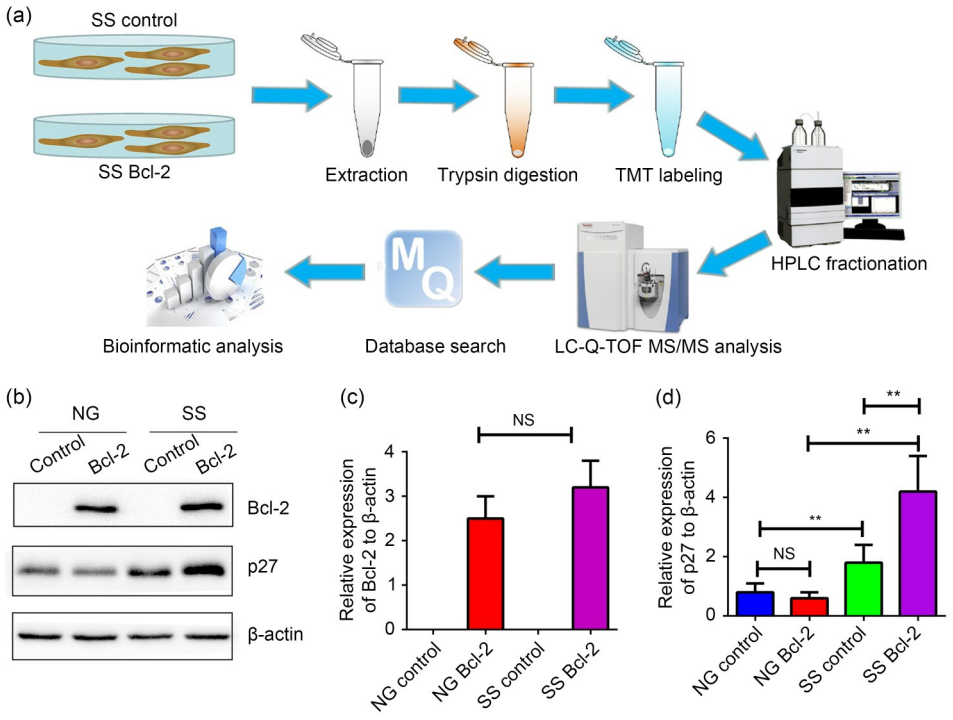

Fig. 1 Overview of the proteomic analysis of the Bcl-2 cells subjected to serum starvation (SS). (a) Schematic outline of the workflow of the quantitative proteomic analysis. (b) Western blotting results of Bcl-2 and p27 expression in Bcl-2-overexpressing NIH3T3 cells subjected to normal growth (NG) and SS. (c, d) Quantification of Bcl-2 protein (c) and p27 protein (d) expression. The data are expressed as mean±standard deviation (SD), n=3. ** P<0.01; NS: not significant. Control: transfected vector alone; Bcl-2: transfected vector with the *Bcl-2* gene; LC-Q-TOF MS/MS: liquid chromatography combined with quadrupole-time of flight tandem mass spectrometry; TMT: tandem mass tag; HPLC: high-performance liquid chromatography.

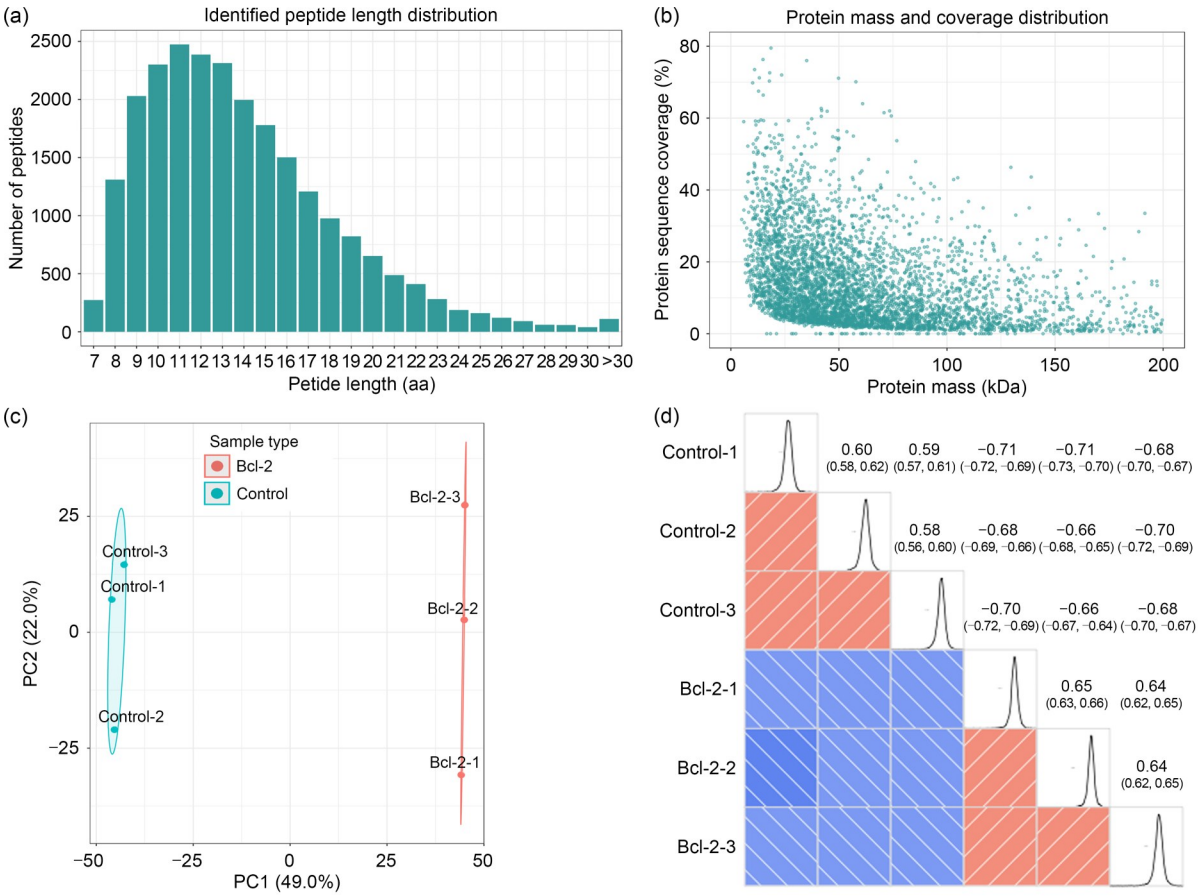

Fig. 2 Analysis of differentially expressed proteins by TMT-based quantitative proteomics. (a) Identification of the length distribution of the peptides by MS; (b) Identification of the relationship between protein mass and coverage by MS; (c) PCA results showing the degree of aggregation between the samples; (d) Heatmap based on Pearson's correlation analysis. TMT: tandem mass tag; MS: mass spectrometry; PCA: principal component analysis; PC: principal component.

proteins yield higher numbers of peptides after digestion, and more peptides have to be identified to achieve the same coverage. The PCA results showed significant differences between the control and Bcl-2 groups, and there was a good repeatability within the groups (Fig. 2c). The Pearson's correlation coefficients between the two groups were low (Fig. 2d), confirming that the proteomic dataset is appropriate for the experiment and meets the required standards. These results indicated that the distribution of the peptide lengths complied with the quality requirements.

3.3 Classification of differentially expressed proteins in Bcl-2 and control after serum starvation treatment

In this study, 400 upregulated and 271 downregulated proteins were identified in Bcl-2 cells after SS treatment compared with those in the control cells, based on the 1.3-fold ratio (Bcl-2/control) (Fig. 3a). All differentially expressed proteins were analyzed based on the clusters of orthologous groups (COG) of proteins, as shown in Fig. 3b. These differentially expressed proteins are involved in various signaling pathways such as RNA processing and modification, chromatin structure and dynamics, energy production and conversion, cell cycle control and cell division, nucleotide transport, and metabolism. The subcellular structural localization of differentially expressed proteins was also predicted and classified using InterProScan (http://www.ebi.ac.uk/interpro). The results showed that the differentially expressed proteins are distributed in the cytoplasm (26.38%), nucleus (26.38%), extracellular space (16.99%), plasma membrane (13.71%), mitochondria (10.13%), cytoplasm or nucleus (3.58%) and other sites (2.83%) (Fig. 3c).

Functional clustering analysis of differentially expressed proteins can reveal potential associations and

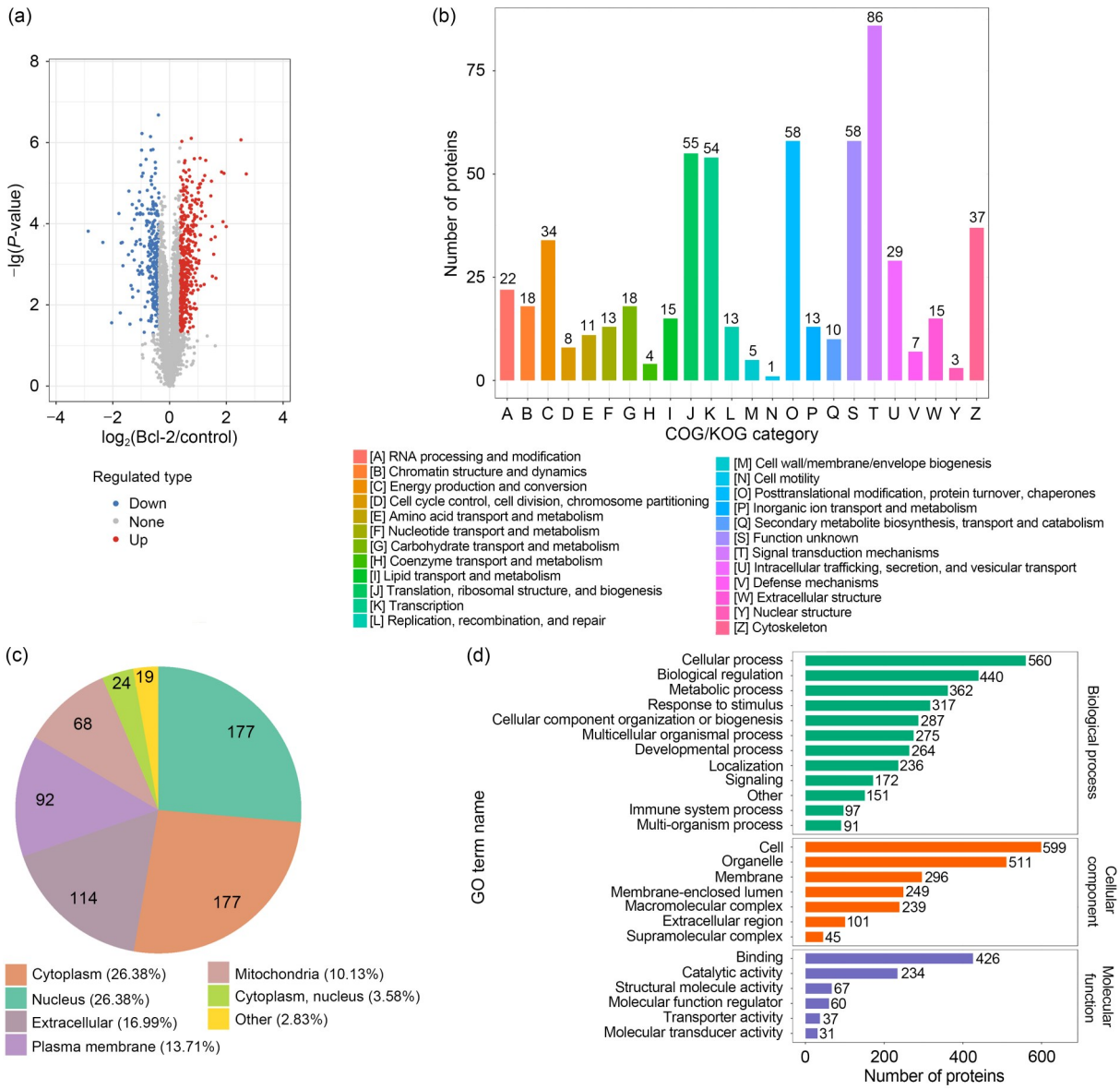

Fig. 3 Classification of differentially expressed proteins in the Bcl-2 and control groups treated by serum starvation (SS). Volcano plot (a), clusters of orthologous groups (COG)/clusters of eukaryotic orthologous groups (KOG) classification (b), subcellular localization and classification (c), and Gene Ontology (GO) classification (d) of differentially expressed proteins.

distinctions between the proteins based on the GO and KEGG pathway databases. GO is an important bioinformatic analysis tool for gene clustering that can classify proteins into tripartite categories, including biological process, cellular component, and molecular function, according to the function of proteins. As shown in Fig. 3d, in the biological process category, the differentially expressed proteins were subclassified mainly into cellular process, biological regulation, metabolic process, response to stimulus, and multicellular organismal process. Numerous differentially expressed proteins were enriched in the detailed processes and pathways, including biological process (Fig. 4a), cellular component (Fig. 4b), molecular function (Fig. 4c), and KEGG (Fig. 4d).

3.4 Functional enrichment and cluster analysis of differentially expressed proteins

To further investigate the important functions of differentially expressed proteins, functional enrichment

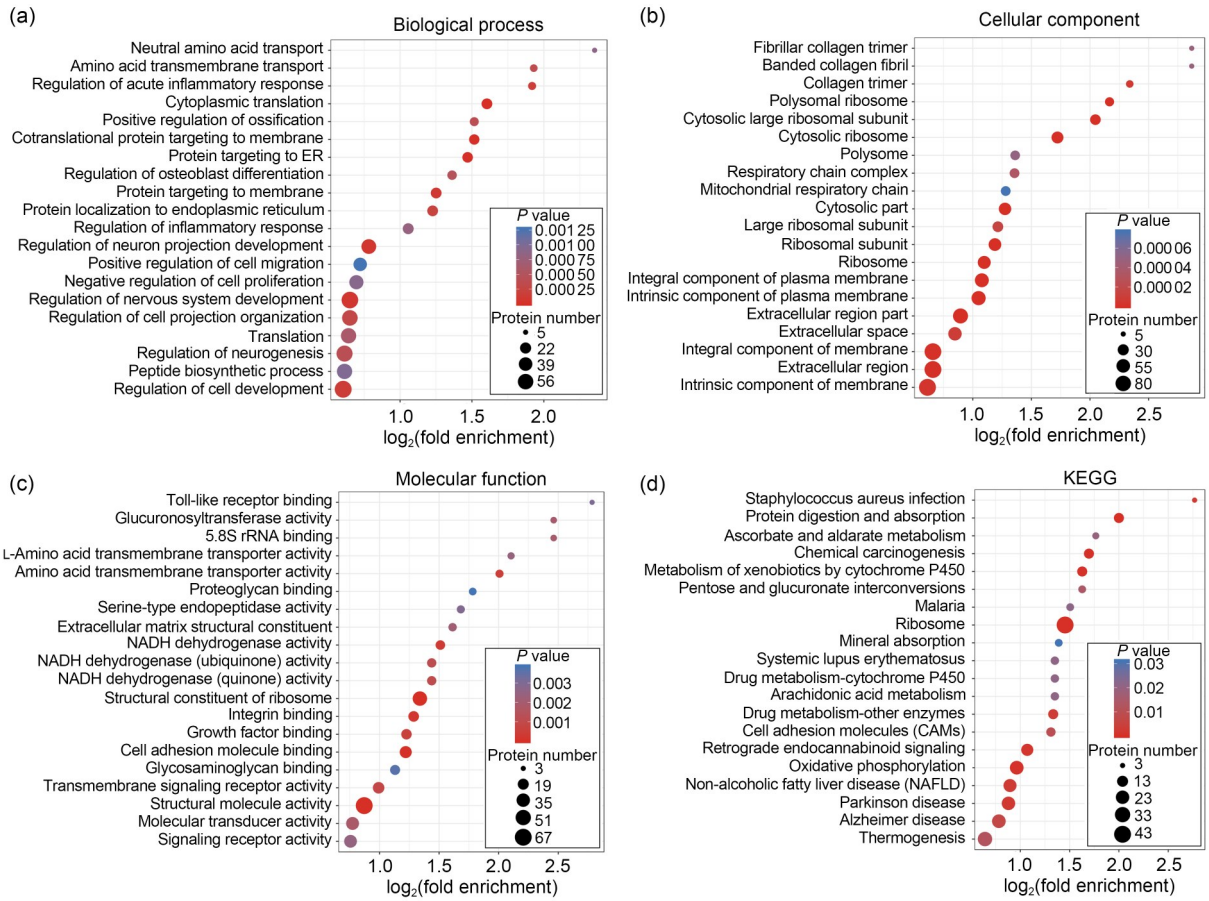

Fig. 4 Bubble charts of differentially expressed proteins enriched in Gene Ontology (GO) and Kyoto Encyclopedia of Genes and Genomes (KEGG). Differentially expressed proteins enriched in biological process (a), cellular component (b), molecular function (c), and KEGG pathways (d). ER: endoplasmic reticulum; rRNA: ribosomal RNA; NADH: nicotinamide adenine dinucleotide.

and cluster analysis were performed. Differentially expressed proteins were analyzed based on 1.3-fold and 1.5-fold changes. The numbers of differentially expressed proteins were 400 (1.3-fold change, upregulated), 271 (1/1.3-fold change, downregulated), 169 (1.5-fold change, upregulated), and 120 (1/1.5-fold change, downregulated), as shown in Fig. 5a. Differentially expressed proteins were divided into quartiles based on the fold change (Bcl-2 vs. control) of differential expression, including <0.667 (1/1.5), 0.667–0.769 (1/1.3–1/1.5), 1.3–1.5, and >1.5 (Table 1). Then, GO, protein domain, and KEGG enrichment analyses were performed, and the results were presented in heatmaps. In the biological process category (Fig. 5b), alternative messenger RNA (mRNA) splicing, regulation of glycogen metabolic process, and mitochondrial calcium ion homeostasis were enriched in the <0.667 group, and pyridine nucleotide biosynthetic process and nicotinamide nucleotide biosynthetic process were enriched in the 0.667–0.769 group, suggesting that Bcl-2 downregulated the proteins of these pathways. Actin filament bundle assembly and striated muscle cell differentiation were enriched in the 1.3–1.5 group, and the respiratory electron transport chain and response to nutrients were enriched in the >1.5 group, suggesting that Bcl-2 upregulated the proteins of the actin filament bundle and electron transport chain pathways. In the cellular component category (Fig. 5c), polymeric cytoskeletal fiber, endoplasmic reticulum, and euchromatin were enriched in the <0.667 group, and cell junction and small subunit processome were enriched in the 0.667–0.769 group, suggesting that Bcl-2 downregulated the proteins of these pathways. The plasma membrane receptor complex was enriched in the 1.3–1.5 group, and the extracellular matrix was enriched in the >1.5 group, suggesting that Bcl-2 upregulated the proteins of these

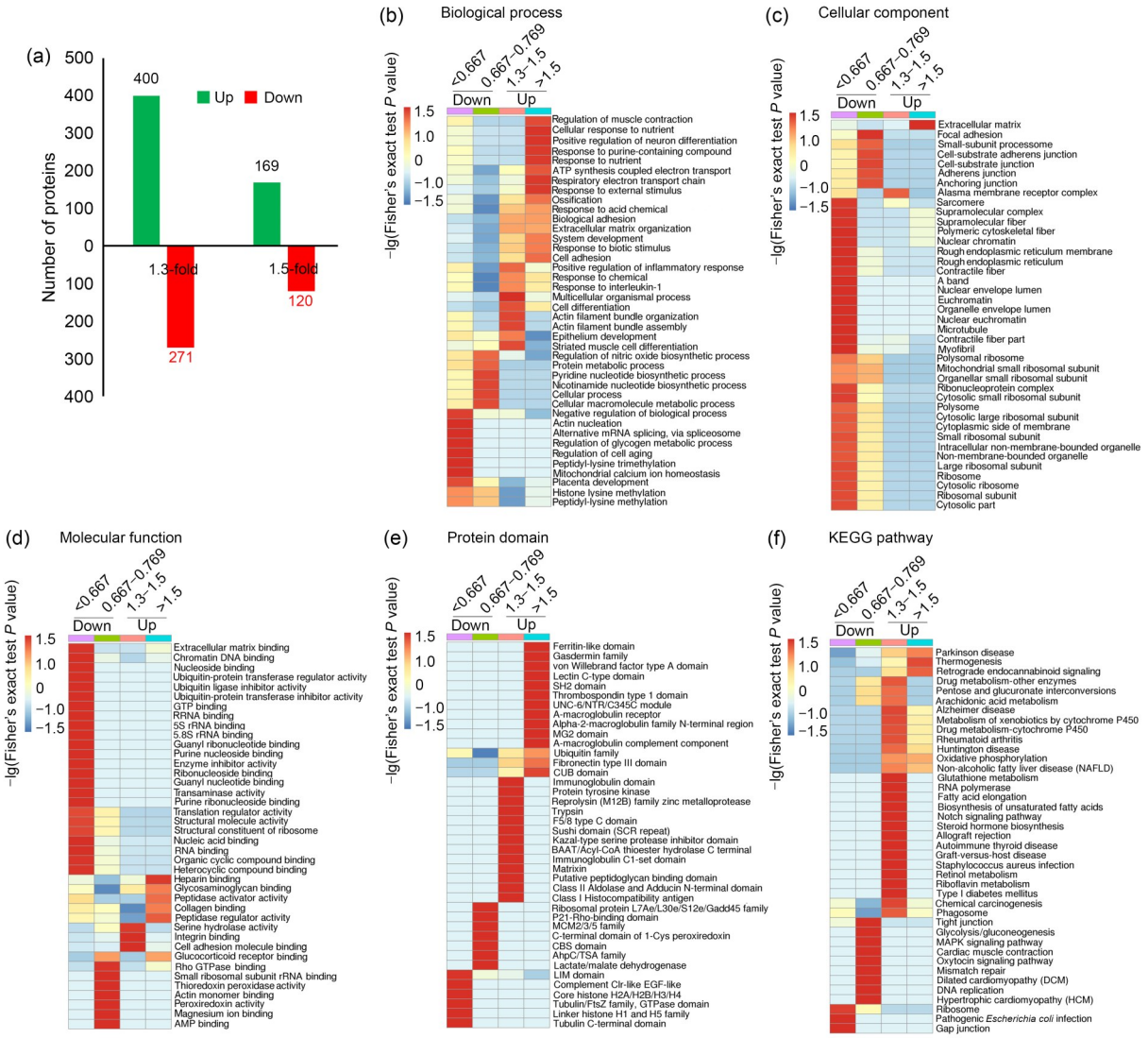

Fig. 5 Functional enrichment and cluster analysis of differentially expressed proteins in the Bcl-2 and control groups treated by serum starvation (SS). (a) Numbers of differentially expressed proteins based on 1.3- and 1.5-fold changes. Biological process (b), cellular component (c), molecular function (d), protein domain (e), and Kyoto Encyclopedia of Genes and Genomes (KEGG) pathway (f) enrichments of differentially expressed proteins. ATP: adenosine triphosphate; mRNA: messenger RNA; GTP: guanosine triphosphate; rRNA: ribosomal RNA; GTPase: guanosine triphosphatase; AMP: adenosine monophosphate; SH2: sperm hammerhead 2; UNC-6: netrin unc-6; NTR: NADPH-thioredoxin reductase; MG2: hypothetical protein; CUB: currant bun; M12B: metallopeptidase; SCR: sex combs reduced; BAAT: bile acid-CoA: amino acid *N*-acyltransferase; Acyl-CoA: acyl-CoA dehydrogenase; MCM: ATPase; Cys: cysteine; CBS: cystathionine β-synthase; AhpC: alkyl hydroperoxide reductase; TSA: tryptophan synthase α chain; LIM: protein lin-11, ISL1 transcription factor and mechanosensory protein 3; Clr: calcitonin receptor; EGF: epidermal growth factor; FtsZ: filamenting temperature-sensitive mutant Z.

pathways. In the molecular function category (Fig. 5d), the pathways of ribosome binding, ubiquitination, and aminotransferase were enriched in the <0.667 group, and the pathways of ribosomal RNA (rRNA) binding and peroxiredoxin activity were enriched in the 0.667–0.769 group, suggesting that Bcl-2 downregulated the proteins of these pathways. The pathways of serine hydrolase activity and cell adhesion molecule binding were enriched in the 1.3–1.5 group, and glycosaminoglycan binding and peptidase regulator activity were enriched in the >1.5 group, suggesting that Bcl-2 upregulated the proteins of these pathways. These differentially expressed proteins enriched in GO terms are listed in Table 2.

Table 1 Differentially expressed proteins classification of 1.3- and 1.5-fold changes

Fold change		Proteins
Down	<0.667	Lmod1, Tubb6, Fhl1, Rbl1, Myh11, Hmgn5, Rpl18, Rpl15, Sox12, Cyb5b, Ccn1, Grpel2, Krt76, Dnd1, Tagln, Bcl2l13, Rpl6, Plgrkt, Rpl14, Ran, Mbnl2, Rpl10a, Coq7, Cycs, Rpl35, Csrp1, Rpl29, Lyar, Ssr3, Dhrs1, Pawr, Asns, Mrps21, Ncbp2, H1-4, Atp2b4, H1-2, Palld, Itga7, Srsf6, Rps24, Nid1, Nme1, Sorbs1, B2m, Kyat3, Rps25, Mrpl16, Mcub, Fbln2, Clk3, Elp3, H2ac20, Katnal2, Rpl11, Mark3, Mrps33, H1-0, Txnip, Arl3, Uba52, Pes1, H3c2, Rpl19, Arpc4, Tes, Ublcp1, Tagln2, Ptgs2, Tomm22, Tgfb1i1, Rpl38, Uchl3, Rrp9, Grb10, Rps6ka3, Tuba1b, Tgm2, Tubb5, Rps8, Dcn, Aacs, Map4k1, Rpl28, Pnisr, Ezh2, Hspe1, Plekhh2, Mrps5, Aldh2, Rpl7, Drg2, H1-5, Grn, Nudt12, Atp5mf, Arl6ip5, Slfn9, Dad1, Rpl26, Rpl4, Tmed4, Gadd45gip1, Phox2b, Cacybp, Lmf2, Clec4f, Nectin1, Rps9, Rpl13a, Fh, Rps23, Tubb2b, Cox4i1, Rps7, Rps27l, H2bc12, Slu7, Gspt1, Tjp2
	0.667–0.769	Cd109, Lpp, Afg3l1, H4c1, Sfxn1, Mrps31, Rpl27, Clasp2, Triap1, Znf608, Cdc42ep3, Sfxn2, Ccdc88b, Tulp3, Prkaca, Ythdc1, Rfc5, Senp1, Ankzf1, Rfc1, Mcm7, Mrps11, Filip1l, Coro1c, Top2a, Mmut, Thy1, Tmlhe, H3-3a, Vcan, Itgb6, Abhd11, Uqcrfs1, Cav1, Cbwd1, Gapdh, Prkag1, Ngdn, Rps18, Rpl31, Cers4, Impdh2, Rpl18a, Imp3, Eif3f, Clybl, Pdlim5, Ldhb, Gpatch4, Aars2, Smad3, Rpl30, Mcm4, Cnbp, Ndufa4, Mrps23, Apool, Hspa2, Rps15a, Cxxc1, Zfyve27, Mrps16, Ssbp1, Septin10, Rps21, Upp1, Armcx1, Cacna2d1, Ppp2r2a, Rpl34, Anxa3, Ano10, Kif13a, Utp18, Prdx3, Myl6, Pgk1, Slc25a24, Pelo, Fdps, Mdh2, Atl2, Psmd13, Ugdh, Ehd2, Pla2g4a, Rab1b, Dstn, Pfkl, Hgf, Abce1, Vasp, Prps2, Nsd3, Jpt2, Rpl24, Ercc6l, Pgam5, Phb, Rpl36a, Mrto4, Timm44, Htra2, Tmsb10, Rpl13, Tpm3, Prdx2, Hsd11b1, Ola1, Rpl7a, Fam210a, Tecr, Ppid, Pak1, Rps13, Srsf10, Metap1, H1-3, Nop2, Dnajc7, Mta2, Rpl35a, Ep400, Prrx1, Ywhah, Tnpo2, Rnf25, Rpl10, Msn, Gusb, Bmp1, Myh10, Eif1ax, Cox6c, Ptgis, Spcs1, Idi1, Znf281, Ddx56, Gak, Gfpt1, Dock7, Polr1c, Ilk, Pdia6, Oga, Map2k3, Pfn2, S100a4, Igf2bp1, Pon3
Up	1.3–1.5	Synpo, Maged1, Lrrc8a, H2-D1, Polr2h, Cert1, Ubl5, Znf503, Triobp, Tars1, Slc6a9, Entpd5, Fut11, Adam23, Phldb1, Ubqln4, Btf3l4, Ess2, Ndufa13, Brdt, Tsnax, Atp9b, Enpp1, Tollip, Adsl, Dhcr24, Cav2, Rb1cc1, Srbd1, Fads1, Ddah2, Sirt2, Nfib, Tax1bp1, Rdh10, Oxr1, Ndufb11, Ddi2, Gdpd1, Armc6, Foxp1, Vps13c, Ndufs2, Apip, Tmem115, Neo1, Dnajc25, Epn1, Scamp3, Acp2, Slc31a1, C1sa, Shprh, Mcat, Cbr1, Gmppb, Acot5, Crocc, Cers5, Fgfr1, Mgat2, Stau2, Fcgrt, Rab9a, Flnb, Ndufv2, Mesd, Crtap, Cox6b2, Zmpste24, Gpr158, Unc45a, Wls, Comt, Shank3, Ski, Nptn, Kiaa0100, Mmp2, Mdfic, Mxra7, Ccnt1, Taf5, Klhl1, Ugt1a6, Larp4b, Gas7, Sub1, Tmf1, Aph1a, Ppt1, Adprs, Adamts4, Spag5, Ddr2, Cyb5r3, Fhl2, Ngly1, Polr2d, Cxcl12, Enpp4, Pbxip1, Lox, Metap2, Hmga1, Atp6v1b2, Itgb5, Saa3, Hirip3, Tlr2, Atp6v1h, Gas1, Pdlim2, Il1rap, Golga4, Hexim1, Ext2, Src, Rcn3, Tars3, Bzw1, Cul4b, Helq, Med22, Dnajb9, Dyrk1b, Gba2, Ndufa7, Slc33a1, Mark1, Iqcg, Tmem119, Purb, Agrn, Gpx1, Chrac1, Asap1, Scfd1, Colec12, Ncstn, Apex1, Golga1, Galk2, Psen1, Asf1a, Cyhr1, Heyl, Sp110, Adgra2, Osmr, Npc2, Ppfia2, Mtarc2, Fstl1, Rida, Ndufa11, Trim27, Mmp14, Ddt, Brox, Rab6b, Gstm1, Jtb, Abhd14b, Tpp2, Tom1, Acot2, Leprot, Psap, Hdgfl3, Pck2, Cbx6, Rab10, Sigmar1, Plcl2, Mfge8, Tmem165, Efl1, Chsy1, Cd9, Wdr24, Cbr2, Lxn, Flrt3, Mpdz, Uqcrh, Ifi204, Ifi30, Parp3, Rbbp9, Ero1a, Fancm, Ugt2b17, Cdc40, Pdgfra, Gstm2, Col4a2, Ptprg, Col5a1, Polr1e, Add1, Acyp1, Add3, Slc7a5, Itm2c, C1ra, Gbp2, Nisch, Dap, Fam25c, Cplx4, Ipo13, Zscan26, Akr1a1, Bzw2, Rbm42, Ciao3, Slc29a1, Mpst, Rrm1, H2-K1, Rogdi, Gdap2, Ccpg1, Yif1b, Scarf2, Vat1, Rab22a, Zfp37, Ndufa8, Plpp3
	>1.5	Cp, Thbs2, Lpar1, Fancd2, Nrp2, Tmem97, Slc6a6, Fkbp11, Fam171a2, Cirbp, Coa5, Timp2, Ostm1, Itih1, Kif3c, Sdc2, Col1a1, Gpc6, Gvin1, Bag5, Gramd4, Setd1b, Col1a2, Rprd1b, Prr12, Fzd1, Plekhb2, Bag1, Ndfip1, Drap1, Chtf8, Ncor2, Nek5, C3, Tchp, Lamp1, Pcolce2, Gsdmdc1, Gas2, Cnnm2, Mt1, Atrn, Pmf1, Ctbs, Tinagl1, Vps26b, P2rx4, Casp8ap2, Ncor1, Atp1b1, Inppl1, Ppcs, Glmp, Phka1, Plxnb2, Clec2d, Tns2, Cog5, Ndufv3, Plscr3, Poldip3, Cd99, Ndufaf3, Ndufa5, Bcs1l, Lancl1, Ebag9, Vav1, Sass6, Ndufb6, Trip10, Cops7b, Dnajc5, Lgals3bp, Il6st, Ubtd1, Rnf149, Plcd1, B3glct, Serinc3, Aldh1l2, Efcab6, Aqp1, Sparc, Iah1, Hydin, Gmpr2, Cebpb, Zc2hc1c, Ndufs4, Tnfrsf23, Gpc4, Slc35f6, Ephb3, Cxcl5, Kif20a, P3h1, Ghr, Prox1, Col5a2, Uty, Ttc33, Cpne2, Itm2b, Arel1, Ndufb4, Ly6a, Slc7a1, Slc1a5, Isg15, Gsta4, Zfp91, Ttc8, Pnpla8, Mrgprf, Calcoco1, Col12a1, Spn, Adamts1, Mtnd3, Sdcbp, Nde1, Lgals9, Mccc1, Nid2, Gsdmc, Sod1, Fth1, Slc5a3, Erap1, Ube3d, ATP5IF1, Bex6, Ptn, Sqstm1, Marcks, Pzp, Ndufa3, Crabp1, Gpnmb, Pttg1ip, Steap4, Arhgef10, FRRS1, Atp6v0d1, Slc38a2, Wdr81, Tmem106b, Spata31, Ifit1, Aldh3a1, Emb, Rnf207, Mecp2, Tmem176a, Cr1l, Col3a1, Nadk2, Cd82, Ifitm3, Slc16a6, Atf1, Klhdc8b, Setd1a, Cyp2f2, Mindy1, Ftl1, Znf385a, Eif4a2

Table 2 Gene Ontology (GO) classification of differential proteins

GO term description	Related proteins
Cellular component	
Intrinsic component of plasma membrane	Il6st, Flrt3, Spn, Cd9, Itgb6, Gas1, Fgfr1, Aph1a, Slc31a1, Ephb3, Slc38a2, Sorbs1, Tollip, Shank3, Steap4, Thy1, Slc6a9, Emb, Sdcbp, Lancl1, Clec2d, Lpar1, Mrgprf, Ncstn, Ddr2, Osmr, Itga7, Mmp14, P2rx4, Slc5a3, Slc7a1, Psen1, Slc7a5, Atp1b1, Jtb, Enpp1, Itgb5, Htra2, Ghr, Pdgfra, Slc6a6, Tnfrsf23, Plgrkt, Plxnb2, Tlr2, Slc33a1, Cav2, Aqp1, Cav1, Atrn, Cp, Gpc6, Atp2b4, Slc16a6, Cd82, Gpnmb, Tgm2, Plpp3, Slc29a1, Neo1, Nectin1, Ptprg
Integral component of plasma membrane	Slc33a1, Ddr2, Osmr, Itga7, Mmp14, P2rx4, Slc5a3, Slc7a1, Psen1, Slc7a5, Atp1b1, Jtb, Enpp1, Itgb5, Htra2, Clec2d, Ghr, Lancl1, Ncstn, Mrgprf, Pdgfra, Cav2, Aqp1, Cav1, Atrn, Gpc6, Atp2b4, Slc16a6, Cd82, Gpnmb, Plpp3, Slc29a1, Neo1, Nectin1, Ptprg, Plxnb2, Tlr2, Plgrkt, Lpar1, Emb, Il6st, Flrt3, Spn, Cd9, Itgb6, Fgfr1, Aph1a, Slc31a1, Ephb3, Slc38a2, Sorbs1, Tollip, Shank3, Steap4, Thy1, Slc6a9, Sdcbp, Slc6a6, Tnfrsf23
Cytosolic part	Rpl13, Pfkl, Rpl18, Rpl34, Rpl29, Rpl10a, Rpl18a, Rpl24, Rpl35, Rpl4, Rpl36a, Rpl11, Rpl38, Uba52, Rps25, Rps9, Rpl28, Rps18, Rrm1, Rpl6, Rpl35a, Ciao3, Rpl14, Rps13, Rps24, Cyb5r3, Rpl31, Rpl15, Rpl19, Rpl10, Rpl13a, Rpl27, Rpl30, Rps8, Gsdmdc1, Rpl7a, Rps27l, Rps23, Rps21, Rps15a, Rps7, Rpl7
Extracellular region part	Saa3, Sdcbp, Sod1, Thbs2, Wls, Kif20a, C3, Ext2, Ehd2, Hgf, H2-D1, Itm2c, Col5a1, Gbp2, Gsdmdc1, Col1a2, Gstm1, Grn, H2bc12, Col5a2, B2m, Cxcl12, Tinagl1, Gstm2, Cd9, Spn, Flrt3, Cxcl5, Ddt, Adamts1, Col3a1, Gusb, Aqp1, Atrn, Ppt1, Ptn, Lgals9, Pdia6, Ptgis, Crtap, Lgals3bp, Enpp1, Mfge8, Prkaca, Clec2d, Ghr, Il6st, C1ra, H2-K1, Itm2b, Col1a1, Nid2, Agrn, Pon3, Sparc, Col4a2, Vcan, C1sa, Cp, Ccn1, Lox, Col12a1, Nid1, Tgm2, Timp2, Dcn, Ptprg, Mmp2, P3h1, Adamts4, Pgk1, Mmp14, Psap
Molecular function	
Structural molecule activity	Rpl36a, Rpl4, Rpl35, Rpl24, Rpl18a, Rpl10a, Psmd13, Pdlim5, Ndufa7, Rpl11, Rpl29, Rpl18, Rpl13, Rps18, Rpl6, Mrps16, Rpl14, Rpl35a, Rb1cc1, Add3, Rpl34, Rpl38, Uba52, Rps25, Col1a2, Col5a1, Col1a1, Fbln2, Arpc4, Rps8, Rpl30, Rpl27, Rpl13a, Rpl10, Rpl19, Rpl15, Rpl31, Msn, Mrps11, Rps24, Myl6, Rps13, Myh11, Rpl28, Rps9, Vcan, Col4a2, Agrn, Cav1, Crocc, Add1, Cav2, Col3a1, Rpl7, Mrps23, Mrps21, Rps15a, Rps21, Mrps5, Mrpl16, Mrps33, Rps23, Rps27l, Tinagl1, Shank3, Tuba1b, Tubb5
Cell adhesion molecule binding	Tinagl1, Mmp14, Itga7, Timp2, Nectin1, Neo1, Plpp3, Gpnmb, Nptn, Ccn1, Col3a1, P2rx4, Msn, Nisch, Sdcbp, Src, Thy1, Cxcl12, Fgfr1, Col5a1, Ilk, Itgb6, Cd9, Mfge8, Itgb5, Psen1
NADH dehydrogenase activity	Ndufb11, Ndufa3, Ndufs4, Ndufa7, Ndufv3, Ndufa8, Ndufa5, Ndufa13, Ndufb4, Ndufa11, Ndufv2, Ndufb6, Mtnd3, Ndufs2
Amino acid transmembrane transporter activity	Serinc3, Slc6a9, Slc38a2, Slc7a5, Slc7a1, Slc1a5, Slc6a6
Growth factor binding	Gpc4, Col3a1, Pdgfra, Tnfrsf23, Pzp, Sdcbp, Fgfr1, Col1a2, Col5a1, Col1a1, Il6st, Ghr, Nrp2, Ptn, Osmr, Cd109, Agrn
Transmembrane signaling receptor activity	Tnfrsf23, Ephb3, Fgfr1, Fzd1, Fcgrt, Spn, Il6st, Lancl1, Ghr, Clec2d, Nrp2, P2rx4, Ddr2, Mrgprf, Lpar1, Pdgfra, Plxnb2, Ptprg, Sigmar1, Cr1l, Adgra2, Osmr
Biological process	
Cytoplasmic translation	Rpl35a, Rpl6, Rpl18, Rpl10a, Rps7, Rps21, Rps23, Rpl7, Gspt1, Rpl29, Rpl30, Rpl15, Rpl31, Rpl38, Rpl11, Rpl36a, Rpl4, Rpl24, Rpl18a, Rpl19
Protein targeting to ER	Rps18, Rpl10a, Rps7, Rps15a, Rps23, Rps8, Rpl30, Rpl19, Rpl13, Rpl15, Spcs1, Rps9, Rps25, Uba52, Rpl11, Rpl36a, Rpl35, Rpl24, Rps13

To be continued

Table 2

GO term description	Related proteins
Protein targeting to membrane	Sdcbp, Rps23, Rps8, Rpl30, Rpl19, Rpl15, Oga, Rps13, Rps15a, Rps9, Uba52, Rpl11, Rpl36a, Rpl35, Rpl24, Rpl10a, Rpl13, Rps18, Rps25, Rps7
Protein localization to endoplasmic reticulum	Rab10, Rps18, Rpl13, Rpl24, Rps7, Rps15a, Rps23, Rps8, Rpl30, Rpl10a, Rpl19, Rps13, Spcs1, Rps9, Rps25, Uba52, Rpl11, Rpl36a, Rpl35, Rpl15
Regulation of programmed cell death	Src, Prdx2, Rps27l, Prdx3, Slc35f6, Sod1, Znf385a, Tax1bp1, Thy1, Tomm22, Txnip, Tmf1, Cxcl12, Pla2g4a, Dad1, Dnajc5, Vav1, Pttg1ip, Serinc3, Rps7, Bcl2l13, Tnfrsf23, Ddah2, Hspe1, Fgfr1, Srsf6, Ppt1, Apip, Uba52, Pawr, Rpl11, Sp110, Ptgs2, Ndufa13, Rps6ka3, Pak1, Cebpb, Mmp2, Lpar1, Top2a, Sigmar1, Sqstm1, Rb1cc1, Arl6ip5, Psen1, Ppid, Fhl2, Asns, Gas1, Gapdh, Casp8ap2, Ilk, Itm2c, Hgf, Ptn, Ifi204, Foxp1, Il6st, Htra2, Hmgn5, Ptgis, Rpl10, Phb, Lgals9, Gramd4, Oxr1, Tgm2, Sirt2, Cycs, Dhcr24, Maged1, Map2k3, Gpx1, ATP5IF1, Map4k1, Nme1, Mecp2, Ccn1, Dap, Bag1, Ywhah, Agrn, Cav1, Aqp1, Apex1, Trip10, Aldh2, Bag5, Arel1, Smad3
Amino acid transmembrane transport	Slc6a6, Serinc3, Slc6a9, Slc38a2, Slc7a1, Arl6ip5, Slc1a5, Slc7a5
Electron transport chain	Ndufa3, Mecp2, Cox4i1, Cyb5b, Aldh2, Cycs, Ndufs4, Ndufa7, Ndufa5, Ndufs2, Ndufa8, Ugdh, Coq7, Akr1a1, Cox6c, Uqcrh, Mtnd3, Ndufb6, Ndufv2, Ndufb4, Uqcrfs1
Calcium ion homeostasis	Tmem165, Cxcl5, Thy1, Ero1a, Il6st, Mcub, Atp1b1, Psen1, Oga, Plcd1, Pawr, Lpar1, Pdgfra, Tgm2, Smad3, Nptn, Atp2b4, Cacna2d1, Cav1, P2rx4
Oxidation-reduction process	Hsd11b1, Coq7, Ero1a, Gapdh, Fh, Ifi30, Mcat, Akr1a1, Impdh2, FRRS1, Cox6c, Il6st, Ldhb, Mdh2, Fads1, Uqcrh, Mtnd3, Uqcrfs1, Ugdh, Tmlhe, Steap4, Ndufb6, Tecr, Prdx2, Ndufs2, Prdx3, Sod1, Uty, Ndufv2, Pdia6, Mtarc2, Lox, Mecp2, Cp, Cox4i1, Cbr1, Aldh3a1, Cyb5b, Ciao3, Cyp2f2, Cbr2, Aldh1l2, Aldh2, Dhcr24, Cycs, Apex1, Gmpr2, Gpx1, Ndufb4, Ndufa13, Cyb5r3, Rrm1, Ndufa5, Ptgs2, Ndufa8, Pgk1, Ndufa3, Phka1, Ndufs4, P3h1, Pfkl, Adsl, Rdh10, Rb1cc1, Oxr1, Pck2, Ndufa7

NADH: nicotinamide adenine dinucleotide; ER: endoplasmic reticulum.

In addition, protein domain enrichment analysis of the differentially expressed proteins showed that in the <0.667 and 0.667–0.769 groups (downregulation) most of the enriched domains were related to the function of ribosomal protein, peroxisomes, and tubulin. In the 1.3–1.5 and >1.5 groups (upregulation), enriched protein domains were involved mainly in membrane receptors of immunity regulation (Fig. 5e). Furthermore, KEGG enrichment analysis was performed to identify potential regulatory pathways involved in the Bcl-2-induced delay of cell cycle entry. In downregulated differentially expressed proteins in the <0.667 and 0.667–0.769 groups, cellular junction, mitogen-activated protein kinase (MAPK) signaling pathway, ribosome, DNA mismatch repair, and other disease pathways were enriched (Fig. 5f). In upregulated differentially expressed proteins in the 1.3–1.5 and >1.5 groups, oxidative phosphorylation, fatty acid biosynthesis, glutathione metabolism, Notch signaling pathway, and other disease pathways were enriched. These differentially expressed proteins enriched in KEGG are listed in Table 3.

3.5 Investigation of potential mechanisms of cell cycle regulation by Bcl-2

According to the KEGG pathway enrichment analysis, a large proportion of differentially expressed proteins associated mainly with ribosomes and oxidative phosphorylation (Table 3) were changed by Bcl-2 during the cell cycle arrest. This result indicated that Bcl-2 affects RNA polymerase to control the transcription of the downstream cell cycle-associated genes and the oxidative phosphorylation signaling pathway to antagonize energy deficiency during cell cycle arrest induced by SS. The results obtained by analysis of the oxidative phosphorylation KEGG map showed that nicotinamide adenine dinucleotide (NADH) dehydrogenase, cytochrome C reductase/oxidase, and adenosine triphosphatase (ATPase) were affected by Bcl-2 expression. In the case of NADH dehydrogenase, most proteins were upregulated, except Ndufa4, which was downregulated. In the case of cytochrome C reductase, indica-specific protein (ISP) was upregulated and ubiquinol-cytochrome C reductase subunit 6

Table 3 Differential proteins enriched in major Kyoto Encyclopedia of Genes and Genomes (KEGG) pathways

KEGG pathway	Related proteins
Ribosome	Rps25, Rps24, Mrps11, Rpl31, Rpl15, Rpl19, Rpl10, Rpl13a, Rpl27, Rpl30, Rps8, Rpl7, Rpl7a, Mrps21, Rps27l, Rps23, Mrps5, Rps21, Rps13, Rpl28, Rps9, Uba52, Rpl26, Rpl35a, Rpl14, Mrps16, Rpl6, Rps18, Rpl13, Rpl18, Rps15a, Rpl34, Rpl10a, Rpl18a, Rpl24, Rpl35, Rpl4, Rpl36a, Rpl11, Rpl38, Rpl29, Rps7, Mrpl16
Oxidative phosphorylation	Uqcrh, Cox6c, Ndufs4, Ndufa8, Ndufv3, Ndufa7, Ndufb4, Ndufa4, Ndufa3, Ndufb11, Cox4i1, Atp5mf, Cox6b2, Ndufa5, Ndufa11, Ndufv2, Ndufb6, Mtnd3, Ndufs2, Atp6v1h, Atp6v0d1, Uqcrfs1, Atp6v1b2, Ndufa13
Cell adhesion molecules (CAMs)	Vcan, Cd99, H2-D1, Sdc2, H2-K1, Nectin1, Neo1, Spn
Pentose and glucuronate interconversions	Akr1a1, Ugdh, Ugt1a6, Ugt2b17, Gusb
Glycolysis	Aldh3a1, Pck2, Pfkl, Pgk1, Akr1a1, Ldhb, Aldh2, Gapdh
Fatty acid elongation	Acot2, Acot5, Ppt1, Tecr
Steroid hormone biosynthesis	Hsd11b1, Ugt1a6, Ugt2b17, Comt
Purine metabolism	Entpd5, Impdh2, Enpp4, Enpp1, Rrm1, Prps2, Adsl, Gmpr2, Nme1
Pyrimidine metabolism	Nme1, Rrm1, Enpp1, Upp1, Entpd5
amino acid metabolism	Adsl, Asns, Gfpt1, Setd1b, Setd1a, Tmlhe, Ezh2, Nsd3, Aldh2, Aldh3a1, Aldh2, Gpx1, Gsta4, Rrm1, Gstm2, Gstm1
Arachidonic acid metabolism	Gpx1, Ptgs2, Ptgis, Cbr1, Cbr2, Pla2g4a
Pyruvate metabolism	Pck2, Fh, Ldhb, Mdh2, Acyp1, Aldh2
Nicotinate and nicotinamide metabolism	Nadk2, Nudt12, Sirt2, Enpp1
RNA polymerase	Polr1e, Polr1c, Polr2d, Polr2h
Cytokine-cytokine receptor interaction	Cxcl12, Il6st, Il1rap, Ghr, Osmr, Cxcl5
Phagosome	Thbs2, Tubb2b, Tubb6, Atp6v0d1, Atp6v1b2, H2-D1, Colec12, C3, C1ra, Tlr2, Itgb5, Lamp1, Tuba1b, Atp6v1h, H2-K1, Tubb5
Focal adhesion	Col1a1, Itgb5, Itga7, Pak1, Pdgfra, Col4a2, Hgf, Itgb6, Cav1, Cav2, Col1a2, Flnb, Thbs2, Src, Vav1, Vasp, Ilk
Extracellular matrix (ECM)-receptor interaction	Itgb6, Col1a2, Col1a1, Thbs2, Itga7, Itgb5, Agrn, Col4a2
Tight junction	Mpdz, Myh10, Msn, Src, Vasp, Prkaca, Tjp2, Synpo, Tuba1b, Ppp2r2a, Prkag1, Myh11, Myl6
Chemical carcinogenesis	Gsta4, Gstm2, Aldh3a1, Cbr1, Hsd11b1, Gstm1, Ptgs2, Kyat3, Ugt1a6, Ugt2b17
Proteoglycans in cancer	Itgb5, Fgfr1, Src, Sdc2, Prkaca, Fzd1, Flnb, Col1a2, Hgf, Col1a1, Cav2, Cav1, Dcn, Tlr2, Mmp2, Msn, Vav1, Pak1

(QCR6) was downregulated. In the case of cytochrome C oxidase, cytochrome C oxidase subunit IV (COX4) and cytochrome C oxidase subunit 6C (COX6C) were upregulated, and COX6B was downregulated. In the case of ATPase, the F subunit was upregulated, and the B, H, and D subunits were downregulated. These results showed that Bcl-2 regulates ATP synthesis (Fig. 6a). STRING, a database that predicts protein–protein interactions, has been widely used to predict the interactions between known and unknown proteins. All differentially expressed proteins (1.5-fold) and Bcl-2 were searched in the STRING database, and those that are directly related to Bcl-2 are shown in Fig. 6b. The results indicated that Bcl-2 is associated with the indicated proteins in the regulation of cell cycle arrest.

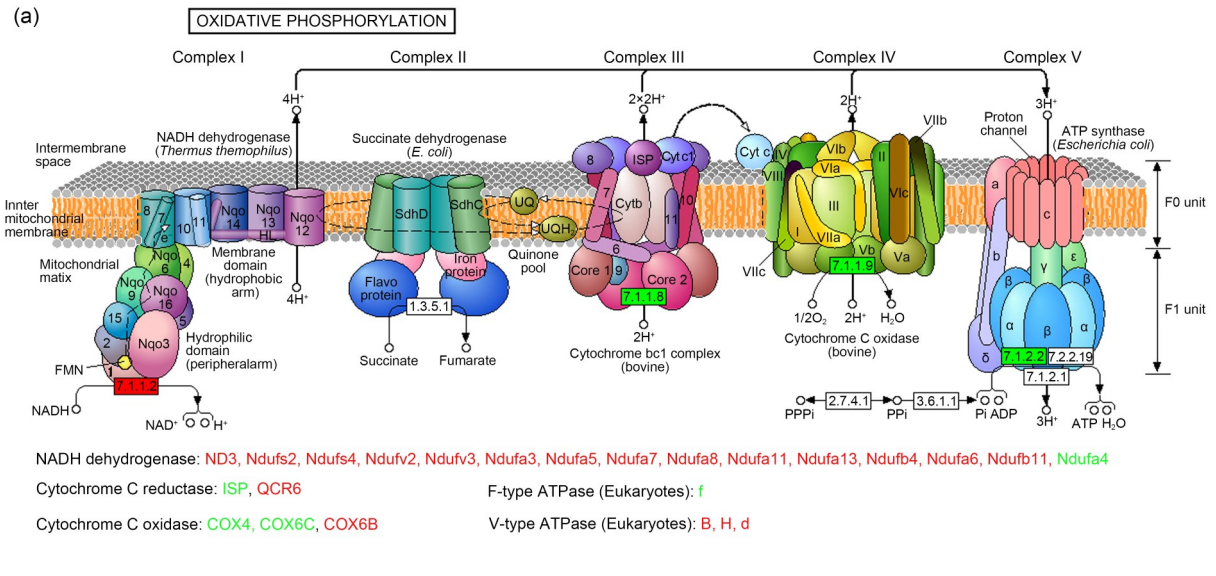

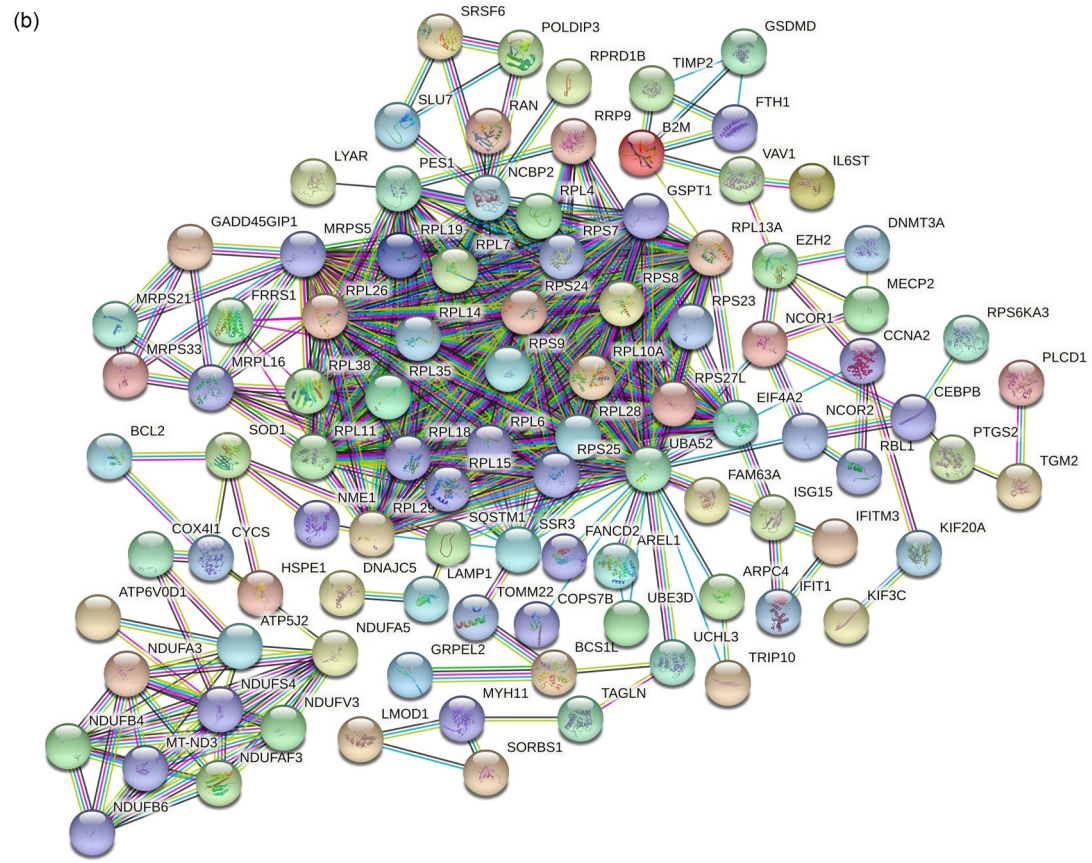

Fig. 6 Mechanism of Bcl-2 regulation. (a) Differentially expressed proteins associated with Bcl-2 regulation of the cell cycle are enriched in the Kyoto Encyclopedia of Genes and Genomes (KEGG) pathway of oxidative phosphorylation. Red indicates upregulation and green indicates downregulation. (b) Interaction analysis of differentially expressed proteins and Bcl-2 using the STRING database. ISP: indica-specific protein; QCR6: ubiquinol-cytochrome C reductase subunit 6; COX4: cytochrome C oxidase subunit IV; COX6C: cytochrome C oxidase subunit 6C; ATPase: adenosine triphosphatase; ND3: mitochondrial NADH-ubiquinone oxidoreductase chain 3; Ndufs2: NADH:ubiquinone oxidoreductase core subunit S2 (Note: for interpretation of the references to color in this figure legend, the reader is referred to the web version of this article).

4 Discussion

Bcl-2 was initially reported as an oncogene translocated and overexpressed in B cell lymphomas (Cleary et al., 1986). Subsequently, Bcl-2 was confirmed to promote cell survival in B lymphocytes, and many proteins homologous to Bcl-2 have been identified. Bcl-2 is located on the outer mitochondrial membrane and regulates Bax/Bak to control mitochondrial fate, protecting permeability of the outer mitochondrial membrane and preventing cytochrome C release and apoptosis (del Gaizo Moore and Letai, 2013). Bcl-2 family proteins not only have well-known apoptotic functions, but also have little-known non-apoptotic functions in processes such as mitochondrial fusion, autophagy, endoplasmic reticulum stress response, and cell cycle regulation (Gross and Katz, 2017; Pandey et al., 2020). Numerous studies have suggested that Bcl-2 family members regulate the cell cycle and may play a critical role in tumor progression (Bonnefoy-Berard et al., 2004; Quinn and Richardson, 2004; Xie et al., 2020). Other studies have shown that Bcl-2 could retard DNA replication fork progression with increased fork asymmetry and lead to DNA replication stress, and that it plays an important role in the progress of the cell cycle (Xie et al., 2014, 2020). We are familiar with the concept that the inhibition of apoptosis is associated with cancer promotion, whereas cell cycle arrest is associated with cancer inhibition. Paradoxically, selected Bcl-2 family members can be both oncogenic and tumor-suppressive. Therefore, various targeted anticancer drugs designed and used for cancer therapy have achieved barely satisfactory clinical outcomes. Such drugs include venetoclax, the first-in-class Bcl-2-specific BH3 mimetic drug (Touzeau et al., 2018). Drug development is a long-term process with high cost and high risk. Although drugs for Bcl-2 protein have been tested, the clinical outcomes are not satisfactory. In this study, proteomics analysis was used in Bcl-2-overexpressing cells after SS treatment to determine the molecular mechanisms or signaling pathways by which Bcl-2 regulates the cell cycle, and to identify suitable targets and strategies for drug development.

SS is a traditional method to synchronize the cell cycle in the G0 phase and has been extensively used in cancer research. The results of the present study indicate that this method is well suited for investigation of the cell cycle synchronization of NIH3T3 cells (Misra et al., 2010; Du et al., 2017). In our previous study, the SS method was used for cell cycle synchronization to demonstrate that Bcl-2 can regulate mitochondrial metabolism by p27 stabilization to produce lower levels of ATP and ROS to enhance G0 quiescence and delay S phase entry (Du et al., 2017). Bcl-2 can arrest the G1/S phase progression and inhibit cyclin E/CDK2 protein kinase activity by increasing the levels of G1 cyclin/CDK inhibitor p27 (Vairo et al., 2000). These results suggested that p27 can be used as a marker for the detection of Bcl-2-dependent blockade of the cell cycle. Our previous study identified a novel mechanistic link between the tumor-suppressive function of Bcl-2 and a reduction in mitochondrial metabolism. However, the detailed effects on mitochondrial metabolism remained unclear. Therefore, to better understand the mechanisms of Bcl-2-dependent delay in cell cycle progression, we investigated the proteomics of Bcl-2-overexpressing cells after SS treatment. In-depth bioinformatics analysis of the proteomic dataset revealed that numerous differentially expressed proteins and the corresponding enriched pathways are likely involved in Bcl-2-dependent delay of the cell cycle. These proteins were identified as being involved in biological processes and cellular signaling pathways. In the present study, GO enrichment analysis of the differentially expressed proteins indicated that these proteins are functionally related to the integral components of the plasma membrane and extracellular region in the cellular component category terms. This result indicated that Bcl-2 can balance the mitochondrial outer membrane integrity disrupted by Bax and protect the plasma membrane from destruction and apoptosis (Kroemer et al., 2007; Delbridge et al., 2016). Bcl-2 family members control cell death primarily by regulating permeability of the mitochondrial outer membrane, leading to the irreversible release of proteins or enzymes from the mitochondria with subsequent activation of caspase, finally resulting in apoptosis. Kale et al. (2018) reviewed Bcl-2 function and the uncertain relationship between Bcl-2 and the plasma membrane. With advances in live cell imaging techniques and the generation of fluorescent recombinant proteins, studies have confirmed that Bcl-2 family proteins not only exist in mitochondria, but also dynamically distribute to other intracellular compartments such as endoplasmic reticulum, Golgi apparatus, nucleus, and peroxisome (Popgeorgiev et al., 2018; Pandey et al., 2020). In our study, the results of GO enrichment analysis revealed that Bcl-2 plays a critical role in cell cycle regulation by affecting the relative gene expression

of the plasma membrane (Table 2), and this hypothesis requires additional investigation. In the case of molecular function, differentially expressed proteins were enriched in structural molecule activity, including mainly ribosomal proteins, cell adhesion, NADH dehydrogenase activity, and transmembrane signaling receptor activity. In the case of biological process, differentially expressed proteins were enriched in translation process, amino acid transmembrane transport, localization to endoplasmic reticulum, calcium ion homeostasis, and oxidation-reduction process. These results indicated that Bcl-2 may affect ribosomes at the translation level to change the expression of the genes related to the enriched pathways. Furthermore, Bcl-2 can regulate mitochondria to influence intercellular signal transduction through endoplasmic reticulum-related pathways. A recent study showed that the ribosomal protein L10 (RPL10) mutation can promote mitochondrial dysfunction, resulting in the accumulation of ROS and a decrease in ATP level in leukemia cells. Such cells can survive via a specific increase in internal ribosome entry site-mediated translation in the case of Bcl-2 overexpression (Kampen et al., 2019). The ribosome plays an important role in delay of the cell cycle induced by Bcl-2 via ATP reduction and ROS accumulation. A previous study demonstrated a close association between Bcl-2 and NADH (Robinson et al., 1998), and the prosurvival function of Bcl-2 is related to its own transmembrane structure (Tanaka et al., 1993). These results suggested potential pathways and associated protein molecules influenced by Bcl-2 regulation of the cell cycle. Although the present study did not determine the detailed mechanism of Bcl-2 regulation of the cell cycle via these potential signaling pathways, the screened key protein molecules provide a basis and a reference for future mechanistic studies.

The KEGG pathway analysis determined that the proteins differentially expressed in the Bcl-2 overexpression group were involved mainly in important cellular pathways, including ribosome, oxidative phosphorylation, glycolysis, phagosome, and various other metabolic pathways. Additional COG/clusters of eukaryotic orthologous groups (KOG) category analysis revealed that Bcl-2-activated differentially expressed proteins that participate in numerous signaling pathways, specifically the cell cycle, involved cyclin T1 (Ccnt1), defender against cell death 1 (Dad1), anoctamin 10 (Ano10), G-patch domain containing 4 (Gpatch4), retinoblastoma-like 1 (Rbl1), NADH:ubiquinone oxidoreductase subunit A13 (Ndufa13), Unc-45 myosin ahaperone A (Unc45A), and cullin 4B (Cul4b) proteins. These proteins may be direct targets of Bcl-2-dependent regulation of the cell cycle. This result indicated that cell cycle-associated proteins were regulated by Bcl-2 at the ribosomal translational level and at the mitochondrial energy supply level. Such proteins require further studies, which may help to understand the regulation of cell cycle by Bcl-2. Ribosomal proteins are the major components of the ribosomes and play an important role in protein biosynthesis. Increasing evidence has demonstrated that a variety of ribosomal proteins participate in cell cycle regulation. Ribosomal protein large Po (RPLPo) can interact with the tumor suppressor gene phospholipase A and acyltransferase 4 (*PLAAT4*) to mediate the expression of cell cycle-associated proteins (Wang et al., 2019). Ribosomal proteins can activate the tumor suppressor pathway independently of p53, and ribosomal protein S14 can act as a CDK4/6 inhibitor linking ribosome biogenesis defects to the main factors responsible for cell cycle progression (Lessard et al., 2019). A study showed that repression of various ribosomal proteins results in arrest at various phases of the cell cycle (Thapa et al., 2013). For example, some ribosomal proteins control the G1 phase and others regulate the G2/M phase, likely because different topological areas of the ribosomes are connected to various modules of the cell cycle (Thapa et al., 2013). Mitochondria are essential for energy conversion in eukaryotic cells and have their own genome to encode some enzymes of oxidative phosphorylation (Hu et al., 2019). These enzymes are synthesized in specialized mitochondrial ribosomes. Therefore, mitochondrial ribosomes are essential for ATP synthesis and ROS production. Additionally, the expression of the genes encoding for mitochondrial ribosome assembly factors and mitochondrial translation factors is associated with tumorigenesis and metastasis of various cancers (Kim et al., 2017). These results in combination with the data of our previous study of Bcl-2-dependent delay of the cell cycle via mitochondrial ATP and ROS indicated that Bcl-2 potentially influences translation of proteins or enzymes of the respiratory chain in the ribosomes and thereby regulates the cell cycle. However, this theoretical hypothesis requires further investigation. In our opinion, the dual role of Bcl-2 in tumors is affected by the tumor microenvironment. The dynamic distribution of related proteins regulated by Bcl-2 in the intracellular membrane system may be involved in the occurrence and development of tumors, but current research cannot fully explain its specific molecular mechanism, and more in vitro and in vivo studies are needed.

5 Conclusions

We identified 169 upregulated proteins and 120 downregulated proteins with a 1.5-fold change and demonstrated the regulatory mechanism of Bcl-2-dependent delay of the cell cycle using TMT-labeled global quantitative proteomic analysis. The differentially expressed proteins were distributed mainly in the cytoplasm and nucleus, and the mitochondria accounted for 10.13% of the proteins. The results of the GO and KEGG enrichment analyses of differentially expressed proteins identified by quantitative proteomics indicated a contribution to the nucleus, ribosome, and oxidative phosphorylation, which may be important for the regulation of the cell cycle by Bcl-2. These proteins may be regarded as targets in screening for anticancer compounds. Additionally, the involvement of multiple differentially expressed proteins in oxidative phosphorylation was confirmed in our previous study that demonstrated that Bcl-2 delays the cell cycle via mitochondrial ATP and ROS (Du et al., 2017). Therefore, additional approaches and strategies will be required to determine the molecular mechanisms of the contribution of differentially expressed proteins to the regulation of the cell cycle by Bcl-2.

Acknowledgments

This work was supported by the Ningxia Higher Education Scientific Research Project (No. NGY2018-69), the National Natural Science Foundation of China (No. 81960480), the Key Research and Development Program of Ningxia (No. 2018BEB04008), and the Ningxia Medical University Scientific Research Project (No. XT2017015), China.

Author contributions

Xing DU, Jingjing XIAO, Bo XU, and Hang HAN performed the experimental research and data analysis. Xing DU and Xufeng FU wrote and edited the manuscript. Yin WANG and Xiuying PEI contributed to the study design, data analysis, and writing and editing of the manuscript. All authors have read and approved the final manuscript and, therefore, have full access to all the data in the study and take responsibility for the integrity and security of the data.

Compliance with ethics guidelines

Xing DU, Jingjing XIAO, Xufeng FU, Bo XU, Hang HAN, Yin WANG and Xiuying PEI declare that they have no conflict of interest.

This article does not contain any studies with human or animal subjects performed by any of the authors.

References

Adams CM, Clark-Garvey S, Porcu P, et al., 2019. Targeting the Bcl-2 family in B cell lymphoma. *Front Oncol*, 8:636. https://doi.org/10.3389/fonc.2018.00636

Bonnefoy-Berard N, Aouacheria A, Verschelde C, et al., 2004. Control of proliferation by Bcl-2 family members. *Biochim Biophys Acta-Mol Cell Res*, 1644(2-3):159-168. https://doi.org/10.1016/j.bbamcr.2003.10.014

Brady HJ, Gil-Gómez G, Kirberg J, et al., 1996. Baxα perturbs T cell development and affects cell cycle entry of T cells. *EMBO J*, 15(24):6991-7001. https://doi.org/10.1002/j.1460-2075.1996.tb01091.x

Cleary ML, Smith SD, Sklar J, 1986. Cloning and structural analysis of cDNAs for *bcl-2* and a hybrid *bcl-2*/immunoglobulin transcript resulting from the t(14;18) translocation. *Cell*, 47(1):19-28. https://doi.org/10.1016/0092-8674(86)90362-4

Delbridge ARD, Grabow S, Strasser A, et al., 2016. Thirty years of BCL-2: translating cell death discoveries into novel cancer therapies. *Nat Rev Cancer*, 16(2):99-109. https://doi.org/10.1038/nrc.2015.17

del Gaizo Moore V, Letai A, 2013. BH3 profiling—measuring integrated function of the mitochondrial apoptotic pathway to predict cell fate decisions. *Cancer Lett*, 332(2):202-205. https://doi.org/10.1016/j.canlet.2011.12.021

Du X, Fu XF, Yao K, et al., 2017. Bcl-2 delays cell cycle through mitochondrial ATP and ROS. *Cell Cycle*, 16(7):707-713. https://doi.org/10.1080/15384101.2017.1295182

Frantzi M, Latosinska A, Mischak H, 2019. Proteomics in drug development: the dawn of a New Era? *Proteomics Clin Appl*, 13(2):e1800087. https://doi.org/10.1002/prca.201800087

Fu XF, Yao K, Du X, et al., 2016. PGC-1α regulates the cell cycle through ATP and ROS in CH1 cells. *J Zhejiang Univ-Sci B (Biomed & Biotechnol)*, 17(2):136-146. https://doi.org/10.1631/jzus.B1500158

Gao SW, Liu F, 2019. Novel insights into cell cycle regulation of cell fate determination. *J Zhejiang Univ-Sci B (Biomed & Biotechnol)*, 20(6):467-475. https://doi.org/10.1631/jzus.B1900197

Gross A, Katz SG, 2017. Non-apoptotic functions of BCL-2 family proteins. *Cell Death Differ*, 24(8):1348-1358. https://doi.org/10.1038/cdd.2017.22

Hatok J, Racay P, 2016. Bcl-2 family proteins: master regulators of cell survival. *Biomol Concepts*, 7(4):259-270. https://doi.org/10.1515/bmc-2016-0015

Hu SY, Zhuang QQ, Qiu Y, et al., 2019. Cell models and drug discovery for mitochondrial diseases. *J Zhejiang Univ-Sci B (Biomed & Biotechnol)*, 20(5):449-456. https://doi.org/10.1631/jzus.B1900196

Janumyan YM, Sansam CG, Chattopadhyay A, et al., 2003. Bcl-xL/Bcl-2 coordinately regulates apoptosis, cell cycle arrest and cell cycle entry. *EMBO J*, 22(20):5459-5470. https://doi.org/10.1093/emboj/cdg533

Janumyan YM, Cui QH, Yan L, et al., 2008. G_0 function of BCL2 and BCL-x_L requires BAX, BAK, and p27 phosphorylation by Mirk, revealing a novel role of BAX and BAK in quiescence regulation. *J Biol Chem*, 283(49):

34108-34120.
https://doi.org/10.1074/jbc.M806294200

Jardim FR, de Almeida FJS, Luckachaki MD, et al., 2020. Effects of sulforaphane on brain mitochondria: mechanistic view and future directions. *J Zhejiang Univ-Sci B (Biomed & Biotechnol)*, 21(4):263-279.
https://doi.org/10.1631/jzus.B1900614

Kale J, Osterlund EJ, Andrews DW, 2018. BCL-2 family proteins: changing partners in the dance towards death. *Cell Death Differ*, 25(1):65-80.
https://doi.org/10.1038/cdd.2017.186

Kampen KR, Sulima SO, Verbelen B, et al., 2019. The ribosomal RPL10 R98S mutation drives IRES-dependent BCL-2 translation in T-ALL. *Leukemia*, 33(2):319-332.
https://doi.org/10.1038/s41375-018-0176-z

Kim HJ, Maiti P, Barrientos A, 2017. Mitochondrial ribosomes in cancer. *Semin Cancer Biol*, 47:67-81.
https://doi.org/10.1016/j.semcancer.2017.04.004

Kroemer G, Galluzzi L, Brenner C, 2007. Mitochondrial membrane permeabilization in cell death. *Physiol Rev*, 87(1):99-163.
https://doi.org/10.1152/physrev.00013.2006

Lessard F, Brakier-Gingras L, Ferbeyre G, 2019. Ribosomal proteins control tumor suppressor pathways in response to nucleolar stress. *Bioessays*, 41(3):e1800183.
https://doi.org/10.1002/bies.201800183

Li FD, Wang YC, Li Y, et al., 2018. Quantitative analysis of the global proteome in peripheral blood mononuclear cells from patients with new-onset psoriasis. *Proteomics*, 18(19):e1800003.
https://doi.org/10.1002/pmic.201800003

Linette GP, Li Y, Roth K, et al., 1996. Cross talk between cell death and cell cycle progression: BCL-2 regulates NFAT-mediated activation. *Proc Natl Acad Sci USA*, 93(18):9545-9552.
https://doi.org/10.1073/pnas.93.18.9545

Misra S, Sharma S, Agarwal A, et al., 2010. Cell cycle-dependent regulation of the bi-directional overlapping promoter of human BRCA2/ZAR2 genes in breast cancer cells. *Mol Cancer*, 9:50.
https://doi.org/10.1186/1476-4598-9-50

Pandey S, Patil S, Ballav N, et al., 2020. Spatial targeting of Bcl-2 on endoplasmic reticulum and mitochondria in cancer cells by lipid nanoparticles. *J Mater Chem B*, 8(19):4259-4266.
https://doi.org/10.1039/d0tb00408a

Pihán P, Carreras-Sureda A, Hetz C, 2017. BCL-2 family: integrating stress responses at the ER to control cell demise. *Cell Death Differ*, 24(9):1478-1487.
https://doi.org/10.1038/cdd.2017.82

Popgeorgiev N, Jabbour L, Gillet G, 2018. Subcellular localization and dynamics of the Bcl-2 family of proteins. *Front Cell Dev Biol*, 6:13.
https://doi.org/10.3389/fcell.2018.00013

Quinn LM, Richardson H, 2004. Bcl-2 in cell cycle regulation. *Cell Cycle*, 3(1):6-8.
https://doi.org/10.4161/cc.3.1.602

Robinson BH, Luo XP, Pitkänen S, et al., 1998. Diagnosis of mitochondrial energy metabolism defects in tissue culture. Induction of MnSOD and bcl-2 in mitochondria from patients with complex I (NADH-CoQ reductase) deficiency. *Biofactors*, 7(3):229-230.
https://doi.org/10.1002/biof.5520070314

Singh R, Letai A, Sarosiek K, 2019. Regulation of apoptosis in health and disease: the balancing act of BCL-2 family proteins. *Nat Rev Mol Cell Biol*, 20(3):175-193.
https://doi.org/10.1038/s41580-018-0089-8

Tait SWG, Green DR, 2010. Mitochondria and cell death: outer membrane permeabilization and beyond. *Nat Rev Mol Cell Biol*, 11(9):621-632.
https://doi.org/10.1038/nrm2952

Tanaka S, Saito K, Reed JC, 1993. Structure-function analysis of the Bcl-2 oncoprotein. Addition of a heterologous transmembrane domain to portions of the Bcl-2β protein restores function as a regulator of cell survival. *J Biol Chem*, 268(15):10920-10926.
https://doi.org/10.1016/S0021-9258(18)82073-7

Thapa M, Bommakanti A, Shamsuzzaman M, et al., 2013. Repressed synthesis of ribosomal proteins generates protein-specific cell cycle and morphological phenotypes. *Mol Biol Cell*, 24(23):3620-3633.
https://doi.org/10.1091/mbc.E13-02-0097

Touzeau C, Maciag P, Amiot M, et al., 2018. Targeting Bcl-2 for the treatment of multiple myeloma. *Leukemia*, 32(9):1899-1907.
https://doi.org/10.1038/s41375-018-0223-9

Vairo G, Innes KM, Adams JM, 1996. Bcl-2 has a cell cycle inhibitory function separable from its enhancement of cell survival. *Oncogene*, 13(7):1511-1519.

Vairo G, Soos TJ, Upton TM, et al., 2000. Bcl-2 retards cell cycle entry through $p27^{Kip1}$, pRB relative p130, and altered E2F regulation. *Mol Cell Biol*, 20(13):4745-4753.
https://doi.org/10.1128/mcb.20.13.4745-4753.2000

Wang CH, Wang LK, Wu CC, et al., 2019. The ribosomal protein RPLP0 mediates PLAAT4-induced cell cycle arrest and cell apoptosis. *Cell Biochem Biophys*, 77(3):253-260.
https://doi.org/10.1007/s12013-019-00876-3

Wang YQ, Liu YH, Wang S, et al., 2020. Hydrogen agronomy: research progress and prospects. *J Zhejiang Univ-Sci B (Biomed & Biotechnol)*, 21(11):841-855.
https://doi.org/10.1631/jzus.B2000386

Warren CFA, Wong-Brown MW, Bowden NA, 2019. BCL-2 family isoforms in apoptosis and cancer. *Cell Death Dis*, 10(3):177.
https://doi.org/10.1038/s41419-019-1407-6

Xie MH, Yen Y, Owonikoko TK, et al., 2014. Bcl2 induces DNA replication stress by inhibiting ribonucleotide reductase. *Cancer Res*, 74(1):212-223.
https://doi.org/10.1158/0008-5472.CAN-13-1536-T

Xie MH, Park D, Sica GL, et al., 2020. Bcl2-induced DNA replication stress promotes lung carcinogenesis in response to space radiation. *Carcinogenesis*, 41(11):1565-1575.
https://doi.org/10.1093/carcin/bgaa021

Xu HD, Qin ZH, 2019. Beclin 1, Bcl-2 and autophagy. *Adv Exp Med Biol*, 1206:109-126.
https://doi.org/10.1007/978-981-15-0602-4_5

Zhou FF, Yang Y, Xing D, 2011. Bcl-2 and Bcl-xL play important roles in the crosstalk between autophagy and apoptosis. *FEBS J*, 278(3):403-413.
https://doi.org/10.1111/j.1742-4658.2010.07965.x